EasyChair Preprint

№ 7756

Detection and Classification of Induction Motor Faults Using DWPD and Artificial Neural Network: Case of Supply Voltage Unbalance and Broken Rotor Bars

Meriem Behim, Leila Merabet and Salah Saad

April 11, 2022

Detection and classification of induction motor faults using DWPD and Artificial Neural Network: case of supply voltage unbalance and broken rotor bars

Meriem Behim
Laboratoire des Systèmes Electromécaniques (LSELM)
Badji-Mokhtar University
Annaba, Algeria
meriembehim96@gmail.com

Leila Merabet
Laboratoire des Systèmes Electromécaniques (LSELM)
Badji-Mokhtar University
Annaba, Algeria
lei_elt@yahoo.fr

Salah Saad
Laboratoire des Systèmes Electromécaniques (LSELM)
Badji-Mokhtar University
Annaba, Algeria
saadsalah2006@yahoo.fr

***Abstract*— It is obvious that time-frequency condition monitoring approaches have known better accuracy when combining it with AI techniques; however, this type of combined techniques is shyly applied, so it needs more encouragement. This article aims to detect and classify induction motor's defects, supply voltage unbalance and broken rotor bars, under several loads, with Artificial Neural Network (ANN), using as indicators: kurtosis and energy values. These values are calculated from Discrete Wavelet Packet Decomposition (DWPD) sub-bands of the stator current signals. The signals are obtained from the simulation of the squirrel cage induction motor (IM). The approach adopted here, is to treat the machine in terms of circuit. The occurred results are discussed.**

***Keywords*— Broken rotor bars, Supply voltage unbalance, Artifitial Neural Network, Kurtosis, Energy, DWPD, Induction motor.**

I. INTRODUCTION

IMs are almost omnipresent in industries. Therefore, many diagnostic techniques are developed to identify the most critical defects occurring on IMs in order to prevent breakdowns, improve the operating time and minimize the shutdown cost. The induction motor defects are expected as: Bearing damages: 42%, Stator winding damages: 28%, Rotor related damages: 8% and other damages: 22%; according to IEEE study results on induction motor defects[1]. To treat and minimize these defects, a multitude of model based approaches and modeless approaches, are developed. Although the latest work is based on the processing of faulty signals using time-frequency methods as short time Fourier transform (STFT), Wigner Ville distribution (WVD) and wavelet transformer (WT) combined with artificial intelligence methods, with the aim of improving fault recognition. However, this type of combined techniques is shyly applied especially when using stator current signals. We cite as references, Bessam et al. [2] (2017) who treat in his article the inter-turn short circuit fault using DWT and NN applied to stator current signal; Zolfaghari et al. [3] (2017) who uses FFT, WPD and multilayer perceptron to detect broken rotor bars through its stator current; Verma et al. [4] (2018) investigated in winding fault using SVM and WT of MCSA; Stator current analysis was exploited also by Haouem et al. [5] (2019) for the diagnosis of faulty current connection using park vector, FT, MSS, park Hilbert and STFT.

This article intended to exploit DWPD and ANN to diagnose and classify broken rotor bars and supply voltage unbalance under several severities and loads using energy and kurtosis as indicators.

This paper is organized as follows: presentation of the machine modeling at section 2. Theoretical background of Discret Wavelet Packet Decomposition, energy and kurtosis are introduced too. Section 3, presents the proposed methodology of this paper. Section 4 is dedicated to the results and classification of fault detection . Conclusion is given in Section 5.

II. MACHINE MODELING

In order to simulate the operation of the system thus controlled, it is imperative to have a model of the machine that can account for its transient behavior during load and voltage variations.

To present the rotor bars individually, the approach adopted here, is to treat the machine in terms of circuit. The rotor is considered as a set of interconnected meshes, each formed by two adjacent bars and the portions of rings that connect them [6]as shown in Fig.1.

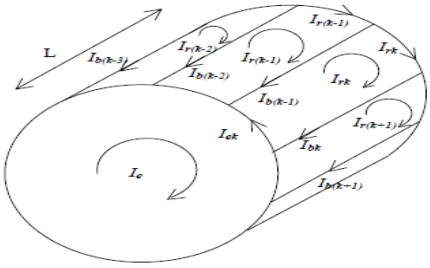

Fig. 1 Rotor structure

The modelisation of broken rotor bars is resumed by the matrix equation [6]:

$$\begin{bmatrix} L_s & 0 & \cdots & \cdots & -M_{sr}\cos ja & \cdots & \cdots & 0 \\ 0 & L_s & \cdots & \cdots & -M_{sr}\sin ja & \cdots & \cdots & 0 \\ \vdots & \vdots & L_{bp}+\frac{2L_e}{N_r}+2L_b & M_r-I_b & M_r & M_r & M_r-I_b & \frac{L_e}{N_r} \\ \vdots & \vdots & M_r-I_b & L_{bp}+\frac{2L_e}{N_r}+2L_b & M_r-I_b & M_r & M_r & \\ \frac{3}{2}M_{sr}\cos ka & \frac{3}{2}M_{sr}\sin ka & & & \ddots & & \vdots & \\ \vdots & \vdots & & & & \ddots & & \\ \vdots & \vdots & M_r-I_b & M_r & M_r & M_r-I_b & L_{bp}+\frac{2L_e}{N_r}+2L_b & \frac{L_e}{N_r} \\ 0 & 0 & \frac{L_e}{N_r} & & \cdots & & \frac{L_e}{N_r} & L_e \end{bmatrix} \frac{d}{dt}\begin{bmatrix} I_{ds} \\ I_{qs} \\ I_{r0} \\ \vdots \\ I_{rj} \\ \vdots \\ I_{r(N_r-1)} \\ I_e \end{bmatrix} = \begin{bmatrix} V_{ds} \\ V_{qs} \\ 0 \\ \vdots \\ \vdots \\ \vdots \\ 0 \\ 0 \end{bmatrix} - \begin{bmatrix} R_s & -\omega L_{ss} & \cdots & \cdots & M_{sr}\omega\sin ja & \cdots & \cdots & 0 \\ \omega L_{ss} & R_s & \cdots & \cdots & -M_{sr}\omega\cos ja & \cdots & \cdots & 0 \\ 0 & 0 & \frac{2R_b}{N_r}+R_{b0}+R_{b(N_r-1)} & -R_{b0} & 0 & 0 & -R_{b(N_r-1)} & \frac{-R_b}{N_r} \\ \vdots & \vdots & & & & & & \\ \vdots & \vdots & 0 & -R_{b(k-1)} & \frac{2R_e}{N_r}+R_{bk}+R_{b(k-1)} & -R_{bk} & 0 & \vdots \\ \vdots & \vdots & & & & & & \\ 0 & 0 & -R_{b(N_r-1)} & 0 & 0 & -R_{b(N_r-2)} & \frac{2R_e}{N_r}+R_{b(N_r-2)}+R_{b(N_r-1)} & \frac{-R_b}{N_r} \\ 0 & 0 & \frac{-R_e}{N_r} & & \cdots & & \frac{-R_e}{N_r} & R_e \end{bmatrix} \begin{bmatrix} I_{ds} \\ I_{qs} \\ I_{r0} \\ \vdots \\ I_{rj} \\ \vdots \\ I_{r(N_r-1)} \\ I_e \end{bmatrix} \quad (1)$$

Where: R_b is the bar resistance, R_e: resistance of the ring portion, L_r: bar inductance, $L_{e:}$ ring portion inductance, L_{sc}: cyclic inductance given by [6]:

$$L_{sc} = \frac{3}{2}L_{sp} + l_{sl} = \frac{6}{\pi}\mu_0 \frac{N_s^2}{ep^2}\mathrm{RL} + L_{sl} \quad (2)$$

L_{rp}: the main inductance of a rotor mesh[6].

$$L_{rp} = \frac{N_r - 1}{N_r^2}\frac{\mu_0}{e} 2\pi \mathrm{LR} \quad (3)$$

M_{rr}: mutual inductance between two meshes, presented as[6]:

$$M_{rr} = -\frac{1}{N_r^2}\frac{\mu_0}{e} 2\pi \mathrm{LR} \quad (4)$$

M_{sr}: mutual stator-rotor inductance[6].

$$M_{sr} = \frac{4}{\pi}\frac{\mu_0}{ep^2} N_s \mathrm{LR}\sin\left(\frac{a}{2}\right) \quad (5)$$

a is the electric angle between two rotor meshes [6]:

$$a = \mathrm{p}\frac{2\pi}{N_r} \quad (6)$$

I_{rk} represents the cell current k and Ibk, the bar current k, with[6]:

$$I_{bk} = I_{rk} - I_{r(k+1)} \quad (7)$$

The electromagnetic torque C_{em} is given by [6]:

$$C_e = \frac{3}{2} pM_{sr}\left\{ I_{ds}\sum_{k=0}^{N_r-1} I_{rk}\sin ka - I_{qs}\sum_{k=0}^{N_r-1} I_{rk}\cos ka \right\} \quad (8)$$

III. THEORETICAL BACKGROUND

1) DISCRET WAVELET PACKET DECOMPOSITION:

This technique generates at each level an approximation coefficient containing low frequencies information, and a detail coefficient containing high frequencies information of the original signal without loss or redundancy of data. The operation can be repeated on several levels and leads to the creation of the tree structure shown in Fig.2 [7], [8].

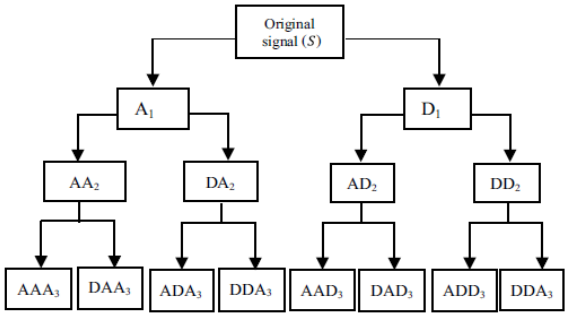

Fig. 2 The tree structure of WPD at depth of 3

2) INDICATORS FOR FAULT DETECTION:

a. ENERGY EIGENVALUES:

The energy represents a strong indicator for fault classification. The energy eigenvalue of each frequency band is defined by[9]:

$$E_j = \sum_{n=1}^{N} |D_j(n)|^2 \quad (9)$$

And the total energy is:

$$E = \sum_{j=0}^{2m-1} |E_j|^2 \quad (10)$$

b. KURTOSIS:

The kurtosis of a signal is defined by the 4th order moment of the amplitude distribution[10].

$$kurtosis = \frac{1}{N}\sum_{i=1}^{N}\left(\frac{x_i - \bar{x}}{\sigma}\right)^4 \quad (11)$$

with: $\bar{x}$: the mean and σ, the sample standard deviation of x_i.

IV. PROPOSED METHODOLOGY

The proposed methodology for this article as shown in the flowchart (Fig.3), consists of four main steps:

Step 1: Data aquisition of simulated broken rotor bars, amplitude and phase shift of voltage unbalance.

Step 2: decomposition of stator current signals into three levels by DWPD using Daubechies mother wavelet (db44).

Step 3: Calculate the energy and kurtosis parameters for the approximations and details of the third level obtained from step 2.

Step 4: Classification of IM defectts using artifitial neural network, by giving both energies and kurtosis as inputs.

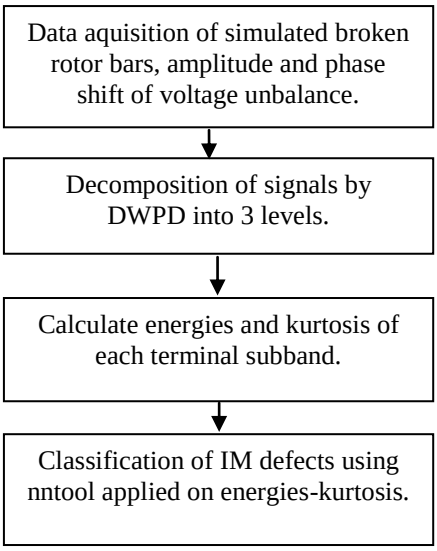

Fig. 3 Proposed methodology

V. RESULTS AND DISCUSSION

1) SIGNAL PROCESSING

In this work, we have simulated a squirrel cage induction motor powered with three voltage sources, and characterized as mentioned in table.1. We have modeled voltage unbalance (in case of amplitude unbalance with 10%, 20%, 30% and 40% and phase shift with 10°, 20°, 30°and 40° on phase A) and rotor bar breakage (one, two, three and four broken bars by replacing the corresponding resistance value by a large value in order to decrease the current that crosses this bar into zero) with an average load of 0, 2 and 3 N.m for both fault types.

Fig.4 represents the three phase currents under a load of 3 Nm, in case of: a) Healthy state, b) 1 broken bar, c) Amplitude unbalance of 10% in phase A, d) phase shift of 10° in phase A.

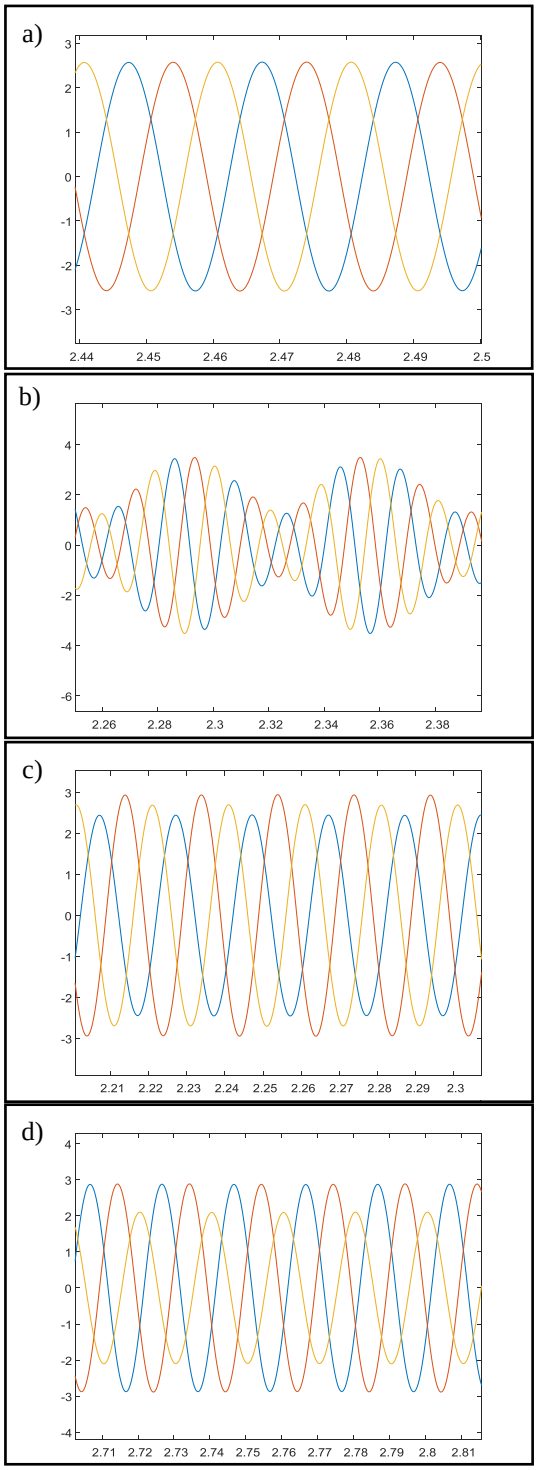

Fig. 4 Three phase current under a load of 3 Nm, in case of: a) Healthy state, b) 1 broken bar, c) Amplitude unbalance of 10% in phase A, d) phase shift of 10° in phase A

Table 1 IM parameters

Stator Resistance	7.828 Ω
Inertia moment	0.006093 Kgm^2
Friction coefficient	0.000725 Nm
pole pairs	1
Rotor bar inductance	10^{-7} H
Short-circuit Leakage inductance	10^{-7} H
Number of bars	16
Number of notches per phase stator	200
Thickness of the air gap	0.00025 m
Length of the machine	0.065m
Average radius of the air gap	0.03575 m
Stator leakage resistance	0.018 H
Rotor bar resistance	$150*10^{-6}$ Ω
Short-circuit Resistance	$72*10^{-6}$ Ω

2) Discret Wavelet Packet Decomposition

The DWPD of the stator current phase is done with Daubechies 'db44' mother wavelet at level 3, as shown in Fig.5, which represents the resultant signals given by the terminal nodes of the DWPD of the stator current, in case of 4 broken bars under a load of 3N.m.

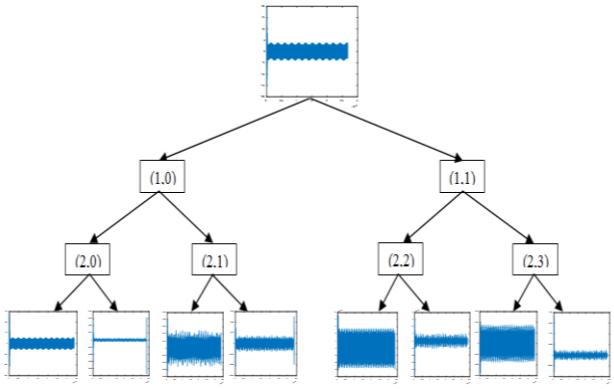

Fig. 5 DWPD of the stator current in case of 4 broken bars under a load of 3 N.m

1) Neural Network:

The proposed indicators used for classification are combination of : energy that is strong but not sensitive enough to incipient defects and kurtosis which is very sensitive to incipient defects but not stable.

As shown by the architecture (Fig.6) of ANN, the classification of the signals is invested according to their types of defects (healthy state, broken bars, supply voltage amplitude imbalance and phase shift of the supply voltage).

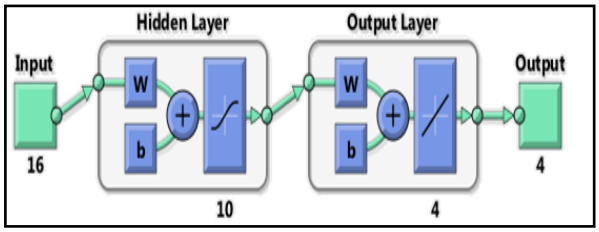

Fig. 6 Neural network architecture

The classification of IM defects is performed by MLP-NN whose parameters are grouped in Table 2.

Table 2 Feed-forward network design parameters

Network input distribution	
Training	66%
Testing	34%
Learning type	Supervised
Activation function	
Hiden layer	Tansigmoid
Output layer	Purlin
Performance	MSE
Weights initialization	Random
Stopped criteria	
Minimum gradient	10^{-7}
Max.Epochs	1000
Mu	0.001
Outputs	Binary

Noting that the classification rate is defined by the ratio of the number of correct classifications to the total number of classification tests:

$$t_r\% = \frac{N_c}{N_t}100 \qquad (12)$$

with: N_c: Number of correct classification and N_t: Number of total tests.

For input vectors composed of energies and kurtosis the performance of the neural network when classifying data made according to the types of defects is worth 92.31%.

VI. Conclusion

This paper is aimed at investigating the two indicators ,energy and kurtosis, in order to classify electrical defects that occurs on IMs using WPD at level 3 and MLP-NN, through the stator current signals. The objective was mostly achieved with a precision of 92.31% (12 out of 13 are correctly classified) with a possibility of improving this result by extending database.

References

[1] S. Kumar et al., « A Comprehensive Review of Condition Based Prognostic Maintenance (CBPM) for Induction Motor », IEEE Access, vol. 7, p. 90690-90704, 2019, doi: 10.1109/ACCESS.2019.2926527.

[2] B. Bessam, A. Menacer, M. Boumehraz, et H. Cherif, « Wavelet transform and neural network techniques for inter-turn short circuit diagnosis and location in induction motor », Int J Syst Assur Eng Manag, vol. 8, no S1, p. 478-488, janv. 2017, doi: 10.1007/s13198-015-0400-4.

[3] S. Zolfaghari, S. Noor, M. Rezazadeh Mehrjou, M. Marhaban, et N. Mariun, « Broken Rotor Bar Fault Detection and Classification Using Wavelet Packet Signature Analysis Based on Fourier Transform and Multi-Layer Perceptron Neural Network », Applied Sciences, vol. 8, no 1, p. 25, déc. 2017, doi: 10.3390/app8010025.

[4] A. K. Verma, S. Radhika, et S. V. Padmanabhan, « Wavelet Based Fault Detection and Diagnosis Using Online MCSA of Stator Winding Faults Due to Insulation Failure in Industrial Induction Machine », in 2018 IEEE Recent Advances in Intelligent Computational Systems (RAICS), Thiruvananthapuram, India, déc. 2018, p. 204-208, doi: 10.1109/RAICS.2018.8635058.

[5] N. Haouem, S. Bouras, A. Bouras, et R. Chemes Eddine, « Experimental investigation for the detection of high-risk external electrical faults through stator current analysis », Australian Journal of Electrical and Electronics Engineering, vol. 16, p. 1-10, avr. 2019, doi: 10.1080/1448837X.2019.1604605.

[6] B. Soumaya, « Contribution à l'amélioration de la sûreté d'exploitation des moteurs à induction. », p. 111.

[7] N. Lahouasnia, M. F. Rachedi, D. Drici, et S. Saad, « Load Unbalance Detection Improvement in Three-Phase Induction Machine Based on Current Space Vector Analysis », J. Electr. Eng. Technol., vol. 15, no 3, p. 1205-1216, mai 2020, doi: 10.1007/s42835-020-00403-y.

[8] H. Bae, Y.-T. Kim, S.-H. Lee, S. Kim, et M. H. Lee, « Fault diagnostic of induction motors for equipment reliability and health maintenance based upon Fourier and wavelet analysis », Artif Life Robotics, vol. 9, no 3, p. 112-116, juill. 2005, doi: 10.1007/s10015-004-0331-7.

[9] M. Gan, C. Wang, et C. Zhu, « Construction of hierarchical diagnosis network based on deep learning and its application in the fault pattern recognition of rolling element bearings », Mechanical Systems and Signal Processing, vol. 72-73, p. 92-104, mai 2016, doi: 10.1016/j.ymssp.2015.11.014.

[10] S. Liu, S. Hou, K. He, et W. Yang, « L-Kurtosis and its application for fault detection of rolling element bearings », Measurement, vol. 116, p. 523-532, févr. 2018, doi: 10.1016/j.measurement.2017.11.049.